COBEM 2023 27TH INTERNATIONAL CONGRESS OF MECHANICAL ENGINEERING

ABCM Brazilian Society of Mechanical Sciences and Engineering
27th ABCM International Congress of Mechanical Engineering
December 04-08, 2023, Florianópolis-SC, Brazil

COB-2023-1054
NUMERICAL ANALYSIS OF THERMAL INSULATION PERFORMANCE IN HEATING PIPE SYSTEMS USING THE FINITE VOLUME METHOD

Diogo Bandeira de Melo Castelo Branco[1]
Lourival Matos de Sousa Filho[2]
[1]Instituto Federal do Maranhão, diogocastelo@acad.ifma.edu.br
[2]Universidade Estadual do Maranhão, lourivalfilho@professor.uema.br

Paulo Roberto Campos Flexa Ribeiro Filho[3]
[3]Universidade Estadual do Maranhão, pauloroberto56@hotmail.com

Abstract. This study investigates the performance of thermal insulation in heating pipe systems by analyzing the thermal and geometric parameters that influence heat flux. The steady-state, one-dimensional heat diffusion equation with constant thermal properties was employed to model the problem. Two boundary conditions were established for the interior: specified temperature and convection. For the exterior, only a convective boundary condition was applied. To solve the differential equation, the finite volume method was employed. The Thomas algorithm was used to address the resulting algebraic equations. The numerical code was implemented on the MATLAB R2022a platform. Different heat transfer coefficients, thermal conductivity, and insulation radius ratios were considered to analyze the impact of these parameters on heat flux. The results indicate that certain configurations intensify heat flux in the insulation for low values of the adopted parameters. Furthermore, assuming the fluid temperature to be the same as the wall temperature (and *vice versa*) is acceptable in specific practical contexts and can be adjusted in the safety factor calculation of the project. Using a dimensionless parameter for insulation thickness proves to be a useful tool for comparing different possibilities in thermal insulation pipe projects.

Keywords Thermal insulation, Critical radius, Finite volume method

1. INTRODUCTION

The critical thickness of insulation plays a significant role in heat transfer analysis. Adding more insulation to a flat surface reduces the rate of heat transfer. However, adding insulation to a cylindrical piece or spherical shell exhibits a different behavior. There is a tendency for an increase in the conduction resistance in the insulation layer and a reduction in the convection resistance due to the increased external area of the convection surface (Çengel, 2009). Understanding temperature distribution serves two key purposes: it aids in optimizing the thickness of insulating materials and helps determine the compatibility between coatings and materials. This temperature distribution is crucial for calculating heat flux within a medium.

The application of thermal insulation is a common practice in duct engineering. However, determining the ideal thickness of insulation is a continually evolving challenge. Li et al. (2012) present a finite volume method based on local analytical solution for the analysis of heat conduction in cylinders. Kaynakli (2014) provides a review of studies related to the determination of the ideal thickness of thermal insulation for pipes and ducts, evaluating the operating conditions and parameters adopted in the listed studies. It also presents studies that aim to determine the optimal insulation thickness in pipes and ducts with various geometries to reduce heat transfer by convection and radiation. Zarubin et al. (2016) study heat transfer through a thermal insulation layer in radiation-convection heat transfer on a non-concave surface, developing a qualitative analysis of the heat flow dependency on the determining parameters for the thermal characteristics of the insulation and its thickness. Shi (2020) presents a methodology for calculating the critical thickness of insulation for an elliptical surface and a dimensionless correlation based on the Biot number. The proposed idea can also be adopted for circular sections after adjusting the geometric parameters accordingly. Anisimova (2020) developed a mathematical model for determining the ineffective thickness of a thermal insulation system, adopting the Newton's method algorithm to calculate the solution to the problem. Usman and Kim (2022) employed computational fluid dynamics to evaluate the optimum insulation thickness based on material and digging costs in South Korea, proposing a micro hybrid district heating (DH) system. Powar and Dhamangaonkar (2022) use the academic version of ANSYS Fluent 19.2 software to perform numerical simulations to estimate the critical thickness of thermal insulation in a circular-geometry duct, adopting the Dirichlet boundary condition for the internal region and the Robin boundary condition for the external region.

In this context, the aim of this work is to present the mathematical and numerical modeling for the phenomenon of heat diffusion in a steady state, unidimensional (r-direction) within a thermal insulator. For the boundary condition of the

inner region, two approaches are considered: specified temperature and convection. For the outer region, only convection is considered. Furthermore, the work proposes the implementation of the code using the finite volumes method in the Matlab software. The study also includes the numerical analysis of the heat flux as a function of the dimensionless parameter "radius ratio" (β), considering the influence of the external convection heat transfer coefficient and thermal conductivity.

2. PROBLEM FORMULATION

The phenomenon under analysis involves a cylinder coated with a thermal insulating material of thickness (e) and thermal conductivity (k). The cylinder has an internal radius (R_{int}) and an external radius (R_{ext}), as illustrated in Figure 1. The external surface is exposed to a flowing fluid with a temperature $T_{f,ext}$ and an external convection heat transfer coefficient h_{ext}. Internally, two cases are considered: in Case 1, the temperature of the inner wall of the tube is specified (T); in Case 2, internal convection is considered, with $T_{f,int}$ representing the temperature of the fluid flowing internally and h_{int} as the internal convection heat transfer coefficient, as shown in Figure 2. Due to the tube's small thickness and high thermal conductivity relative to the insulation, it was neglected in the mathematical modeling.

For the external surface, a convection-type boundary condition is applied, as described by Eq. (1):

$$-k\frac{dT}{dr} = h_{ext}(T(R_{ext}) - T_{f,ext}) \tag{1}$$

For the internal surface, in Case 1, a specified temperature leads to Eq. (2), and in Case 2, convection is taken into consideration, leading to Eq. (3). The corresponding equations are presented below:

$$T = T(R_{int}) \tag{2}$$

$$-k\frac{dT}{dr} = h_{int}(T_{f,int} - T(R_{int})) \tag{3}$$

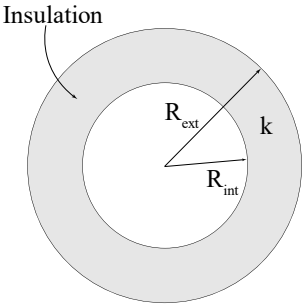

Figure 1. Cylinder diagram (Authors, 2023).

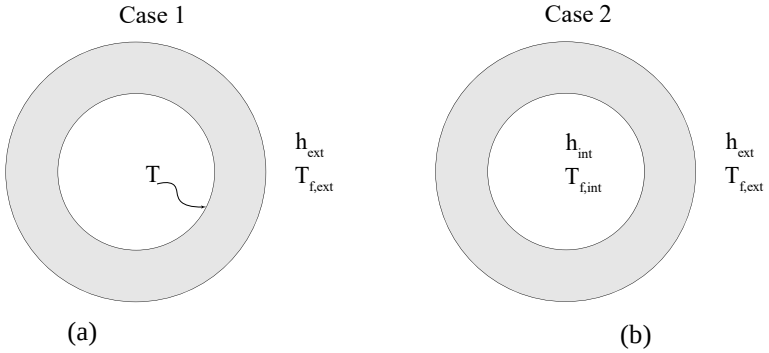

Figure 2. Boundary conditions: (a) Case 1 - Specified internal temperature; (b) Case 2 – Internal convection (Authors, 2023).

3. MATHEMATICAL MODELING

The differential equation of heat diffusion in cylindrical coordinates, considering constant thermal conductivity, one-dimensional problem (radial direction), steady-state, and without internal heat generation, can be written in the form of Eq. (4).

$$\frac{\mathrm{d}}{\mathrm{dr}}\left(\mathrm{r}\frac{\mathrm{dT}}{\mathrm{dr}}\right) = 0 \tag{4}$$

3.1 Analytical Solution

The analytical solution to Eq. (4) is given by Eq. (5), which describes the temperature T as a function of the radius r.

$$\mathrm{T(r)} = \mathrm{C_1}\,\ln|\mathrm{r}| + \mathrm{C_2} \tag{5}$$

The constants $\mathrm{C_1}$ and $\mathrm{C_2}$ can be determined using specific boundary conditions. Table 1 presents the values of these constants for each case under analysis.

Table 1. Values of constants C_1 and C_2 for different boundary conditions (Authors, 2023).

	C_1	C_2
Case 1	$\dfrac{T_{f,ext} - T}{\ln\left(\dfrac{\lvert R_{ext}\rvert}{\lvert R_{int}\rvert}\right) + \dfrac{k}{\mathrm{h_{ext}}\,R_{ext}}}$	$\dfrac{\left(\ln\lvert R_{ext}\rvert + \dfrac{k}{\mathrm{h_{ext}}\,R_{ext}}\right)T - (\ln\lvert R_{int}\rvert)T_{f,ext}}{\ln\left(\dfrac{\lvert R_{ext}\rvert}{\lvert R_{int}\rvert}\right) + \dfrac{k}{\mathrm{h_{ext}}\,R_{ext}}}$
Case 2	$\dfrac{T_{f,ext} - \mathrm{T_{f,int}}}{\ln\left(\dfrac{\lvert R_{ext}\rvert}{\lvert R_{int}\rvert}\right) + \dfrac{k}{\mathrm{h_{int}}\,R_{int}} + \dfrac{k}{\mathrm{h_{ext}}\,R_{ext}}}$	$\dfrac{\left(\ln\lvert R_{ext}\rvert + \dfrac{k}{\mathrm{h_{ext}}\,R_{ext}}\right)\mathrm{T_{f,int}} - \left(\ln\lvert R_{int}\rvert - \dfrac{k}{\mathrm{h_{int}}\,R_{int}}\right)T_{f,ext}}{\ln\left(\dfrac{\lvert R_{ext}\rvert}{\lvert R_{int}\rvert}\right) + \dfrac{k}{\mathrm{h_{int}}\,R_{int}} + \dfrac{k}{\mathrm{h_{ext}}\,R_{ext}}}$

3.2 Numerical Model

Equation (4) was solved numerically using the finite volume method, as described in Patankar (1980), Maliska (2004), and Versteeg and Malalasekera (2007). This method begins by partitioning the problem domain into finite volumes to create a computational grid, illustrated in Figure 3 for a one-dimensional Case. The relationship between grid nodes and interfaces is detailed in Figure 4. Then, the integration of the differential equation for the dependent variable is performed over each volume element. This ensures that the conservation of the involved property is satisfied in each volume element of the grid and, consequently, throughout the solution domain. This procedure results in a system of algebraic equations for each variable of the model. By solving the system of linear algebraic equations, the property distribution of the problem domain is obtained. The system of equations is solved using the Thomas algorithm for one dimension (TDMA-1D), which is considered a direct method for one dimension and an iterative method for two and three dimensions (Maliska, 2004).

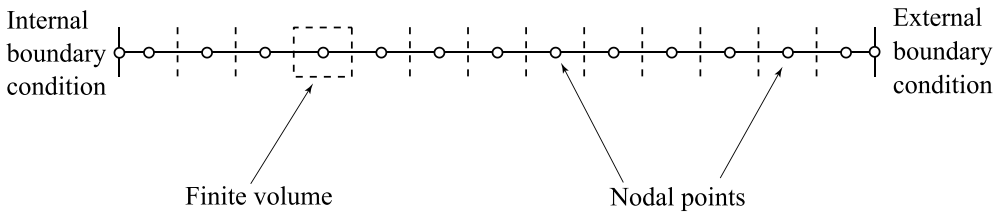

Figure 3. Representation of an elemental control volume in the computational grid within the domain (Authors, 2023).

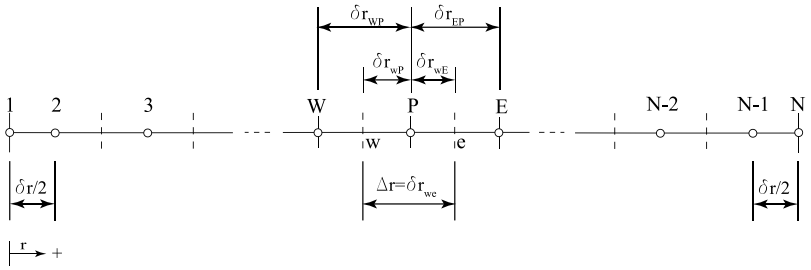

Figure 4. Computational grid (Authors, 2023).

The central difference finite volume scheme (Versteeg and Malalasekera, 2007) was used to discretize the governing equation over control volume P, as shown in Figure 4, and Eq. (4) is transformed into Eq. (9). This transformation process is detailed from Eq. (6) through Eq. (8).

$$\int_w^e \frac{d}{dr}\left(r\frac{dT}{dr}\right)dr = 0 \tag{6}$$

Integrating Eq. (6) over the limits e-w:

$$\int_w^e \frac{d}{dr}\left(r\frac{dT}{dr}\right)dr = r\frac{dT}{dr}\Big|_e - r\frac{dT}{dr}\Big|_w = 0 \tag{7}$$

$$r_e\left(\frac{T_E - T_P}{\delta r_e}\right) - r_w\left(\frac{T_P - T_W}{\delta r_w}\right) = 0 \therefore \left[\frac{r_e}{\delta r_e} + \frac{r_w}{\delta r_w}\right]T_P = \left(\frac{r_e}{\delta r_e}\right)T_E + \left(\frac{r_w}{\delta r_w}\right)T_W \tag{8}$$

The discretized algebraic equation is given by Eq. (9).

$$A_P T_P = A_E T_E + A_W T_W \tag{9}$$

For the volumes corresponding to the boundary conditions, it is given by:

$$A_P T_P = A_E T_E + A_W T_W \text{ (Specified Temperature)} \tag{10}$$

$$A_P T_P = A_E T_E + A_W T_{f,int} \text{ (Convection at the internal surface)} \tag{11}$$

$$A_P T_P = A_E T_{f,ext} + A_W T_W \text{ (Convection at the external surface)} \tag{12}$$

In which the following relation must be satisfied: $A_P = A_E + A_W$

Table 2. presents the coefficients, A_E and A_W, of Eqs. (9), (10), (11), and (12) at their respective nodal points.

Table 2. Temperature coefficients for each volume (Authors, 2023).

	$\mathbf{A_E}$	$\mathbf{A_W}$
1st volume (Specified Temperature)	$\frac{r_e}{\delta r_e}$	$\frac{r_w}{\delta r_w}$
1st volume (Convection)	$\frac{r_e}{\delta r_e}$	$\frac{r_w h_{int}}{k(1+PE)}$
Internal volumes	$\frac{r_e}{\delta r_e}$	$\frac{r_w}{\delta r_w}$
Last volume	$\frac{r_e h_{ext}}{k(1+PD)}$	$\frac{r_w}{\delta r_w}$

Where:

$$PE = \frac{h_{int}\delta r_w}{k} \tag{13}$$

$$PD = \frac{h_{ext}\delta r_e}{k} \tag{14}$$

4. RESULTS AND DISCUSSION

4.1 Numerical Test Data

The data used for the numerical experiment are presented in Table 3. They include the geometric and thermal parameters of the of the studied cases.

Table 3. Parameters used in the calculation (Authors, 2023).

Parameters	Symbol	Value
Internal radius	R_{int}	0.020 m
Radius ratio	β	0.125 – 2.75
Thermal conductivity	k	0.038; 0.043;0.078; 0.1 W/m.K
Internal convection heat transfer coefficient	h_{int}	60 W/m².K
External convection heat transfer coefficient	h_{ext}	2; 16; 25 W/m².K
Wall temperature	T	50 °C
Internal working fluid temperature	$T_{f,int}$	50 °C
External working fluid temperature	$T_{f,ext}$	27 °C

4.2 Critical radius ratio (β_{cr})

The critical insulation radius, Eq. (15), serves as a theoretical reference that indicates the value of the external radius (R_{ext}) of an insulating surface that will yield the maximum heat transfer in a tube, determined by the ratio between the thermal conductivity coefficient (k) of the insulating material and the heat transfer coefficient by convection from the external environment (h_{ext}) (Çengel, 2009).

$$R_{cr} = \frac{k}{h_{ext}} \tag{15}$$

The term β, referred to as the "radius ratio", represents the geometric coefficient calculated as the ratio between the insulation thickness and the internal radius of the tube, as given by Eq. (16).

$$\beta = \frac{e}{R_{int}} = \frac{R_{ext} - R_{int}}{R_{int}} \tag{16}$$

Considering the condition where $R_{cr} = R_{ext}$ and applying it to Eq. (16), the coefficient β_{cr} ("critical radius ratio") is defined, indicating the value of the β coefficient for which there is maximum heat transfer in an insulated cylindrical tube. Therefore, the heat transfer rate from the cylinder increases when $\beta < \beta_{cr}$, is maximum when $\beta = \beta_{cr}$, and decreases when $\beta > \beta_{cr}$. Another application for β_{cr} in thermal insulation cases is its role as a geometric coefficient. Only conditions with $\beta_{cr} \geq 0$ are relevant in the analyses because they indicate that the calculated R_{cr} is greater than the radius of the tube to be insulated.

This study will analyze the heat flux and the effects of insulation thickness based on the value of β. The advantage of using this coefficient lies in evaluating the heat exchange behavior considering the geometric conditions of the analyzed tube and the value of β_{cr} for the tube's operating conditions. It also allows for the comparison of the insulation effectiveness of different geometric conditions.

4.3 Mesh independence

To analyze the influence of the grid on the problem's solution, four grids were tested and compared with the analytical solutions for Cases 01 and 02, as illustrated in Figures 5a and 5b, respectively. The numerical results closely matched the analytical solutions. It was also observed that the finest grid, consisting of 60 volumes, did not yield significantly different results compared to the coarsest grid of 10 volumes, especially when considering processing time. Therefore, the mesh with 40 volumes was selected.

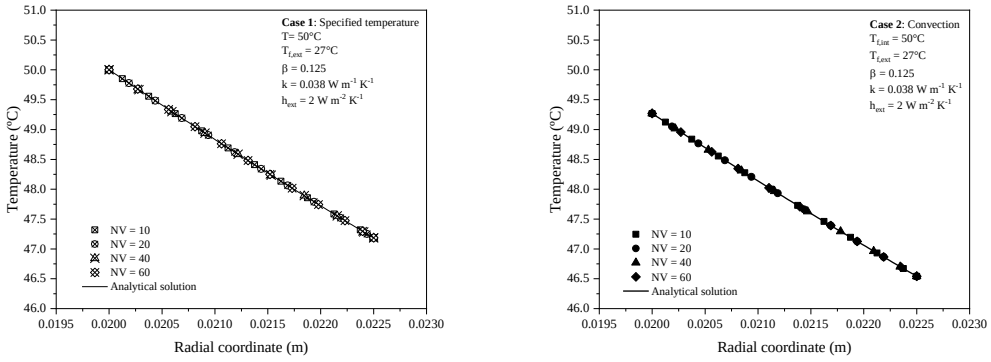

(a) (b)

Figure 5. Grid independence in the problem solution: (a) Case 1; (b) Case 2 (Authors, 2023).

4.4 Results and Analysis

For each case in analysis, simulations were performed by varying β, k, and h_{ext} according to the data provided in Table 3. The results presented in this section were obtained using a computational code developed in the Matlab R2022a platform.

Table 4 presents the critical radii (mm) for the values of k and h_{ext} shown in Table 2. Table 5 provides the corresponding values of β_{cr} for each calculated R_{cr} in Table 4.

Table 4 Critical insulation radius values - R_{cr} (mm) (Autors, 2023).

h (W/m².K)	k (W/ m.K)			
	0.038	**0.043**	**0.078**	**0.1**
2	19.00	21.50	39.00	50.00
16	2.38	2.69	4.88	6.25
25	1.52	1.72	3.12	4.00

Table 5 Critical radius ratio values - β_{cr} (Autors, 2023).

h (W/m².K)	k (W/ m.K)			
	0.038	**0.043**	**0.078**	**0.1**
2	-0.05	0.08	0.95	1.50
16	-0.88	-0.87	-0.76	-0.69
25	-0.92	-0.91	-0.84	-0.80

It can be observed from Table 5 that there are only 3 scenarios in which attention should be given to the effect of undesired increased heat transfer for pipe insulation, which are the cases where $\beta_{cr} \geq 0$.

The temperature distribution in the thermal insulation profile of the tube for various values of β with respect to the internal radius is shown in Figure 6. It can be observed that the temperature profile is no longer linear, as typically seen in a flat plate, but becomes nonlinear, corresponding to a profile in cylindrical coordinates, as the value of β increases. This indicates that the values of β have a direct relationship with the quality of the adopted thermal insulation.

Figures 7a and 7b show the behavior of heat transfer per unit length for Cases 1 and 2, while Figures 7c and 7d show the behavior of heat flux on the external surface of the insulator for both cases, in relation to the variation of β for all values of k presented in Table 3 and $h_{ext} = 2\ W/m^2.K$.

In cases where $\beta_{cr} \geq 0$, an increase in heat transfer per unit length out of the tube is observed when $\beta < \beta_{cr}$, a peak value for $\beta = \beta_{cr}$, and a decrease in heat transfer per unit length for $\beta > \beta_{cr}$. Only one curve in these two cases presented in Figure 7a and 7b exhibits a decreasing heat transfer per unit length behavior for all values of β. This corresponds to the value of $k = 0.038\ W/m.K$, the only one that has $\beta_{cr} < 0$ for all combinations between k and h_{ext}. Figures 7c and 7d show the heat flux on the external surface of the piping. In them, a decreasing trend in heat flux values is observed as β increases. This trend can be explained by the relationship between β and the value of R_{ext}, which consequently influences the value of the external area.

Figure 8 provides a better comparison for significant cases of heat transfer per unit length of $\beta_{cr} > 0$, $k = 0.078 W/m.K$ and $k = 0.1\ W/m.K$.

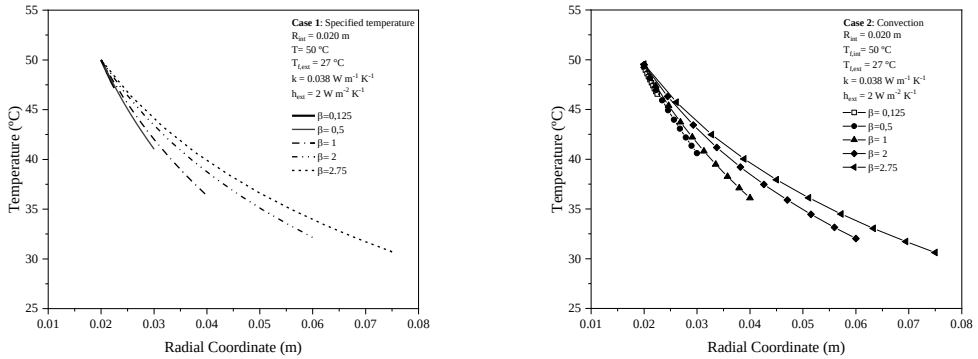

(a) (b)

Figure 6. Influence of β on the temperature profile (Authors, 2023).

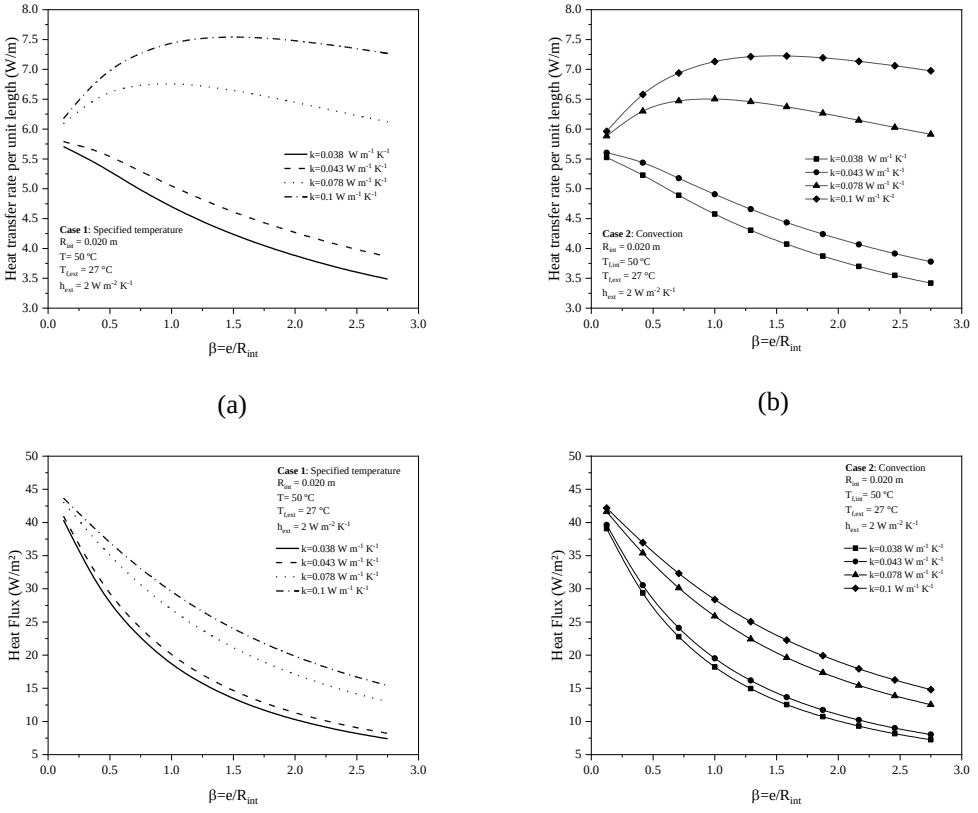

(a) (b)

(c) (d)

Figure 7. Influence of β on the heat transfer per unit length and the heat flux on the external surface for various conductivity coefficients and thermal convection with $h_{ext} = 2\ W/m^2.K$: (a) heat transfer per unit length for Case 1; (b) heat transfer per unit length for Case 2; (c) heat flux for Case 1; (d) heat flux for Case 2 (Authors, 2023).

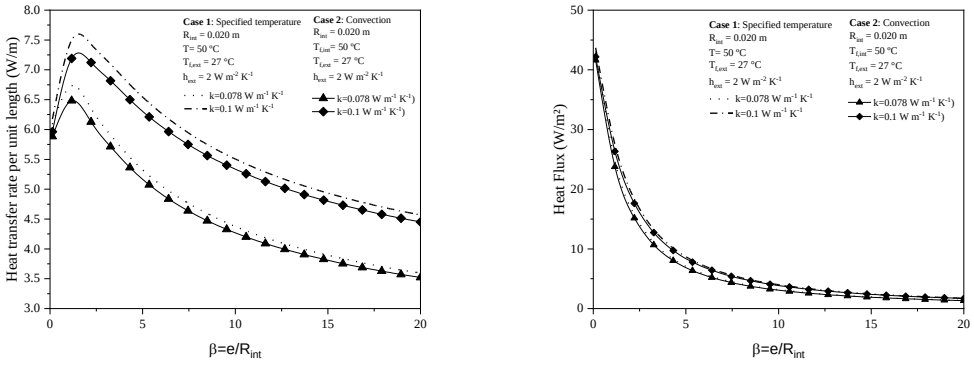

(a) (b)

Figure 8. Comparison of the influence of β on the heat flux on the external surface for significant cases of $\beta_{cr} > 0$ for $h_{ext} = 2\ W/m^2.K$: (a) Heat transfer per unit length (W/m); (b) Heat Flux (W/m²) (Authors, 2023).

Figures 9a and 9b show the behavior of heat flux on the external surface for Cases 1 and 2, respectively, with respect to the variation of β for all values of k presented in Table 3 and $h_{ext} = 16\ W/m^2.K$. They exhibit an effective insulation behavior for all tested values of k, consistent with what is expected since all the β_{cr} values for these cases were negative. This means that, under the simulated condition, there is no risk of reverse heat transfer effects caused by the existence of a critical insulation radius. The difference in heat flux values between the simulated conditions for low values of β is notable, and this difference tends to decrease as the value of β increases. A similar behavior of the heat flux curves is observed $h_{ext} = 25\ W/m^2.K$, as illustrated in Figure 10.

A comparison between the conditions presented in Figures 7a, 7b, 9a, 9b, 10a, and 10b indicates the conservative nature of a heat flux analysis in a tube when the internal convective conditions are disregarded.

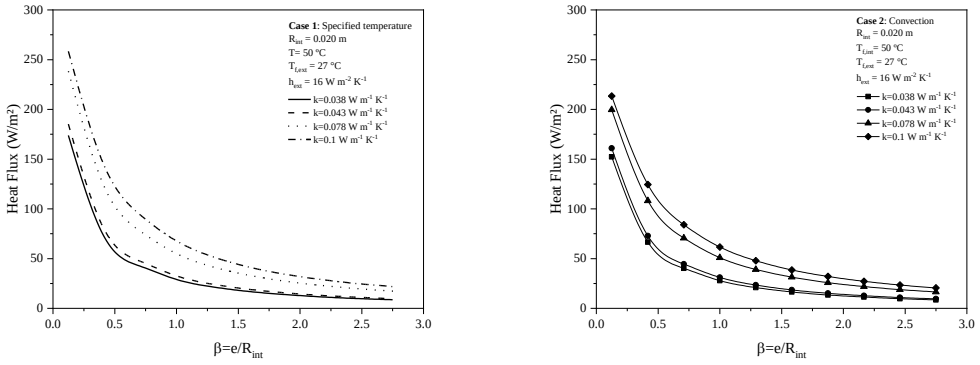

(a) (b)

Figure 9. Influence of β on the heat flux on the external surface for different convective coefficients and thermal conductivities for $h_{ext} = 16\ W/(m^2 \cdot K)$: (a) Case 1; (b) Case 2 (Authors, 2023).

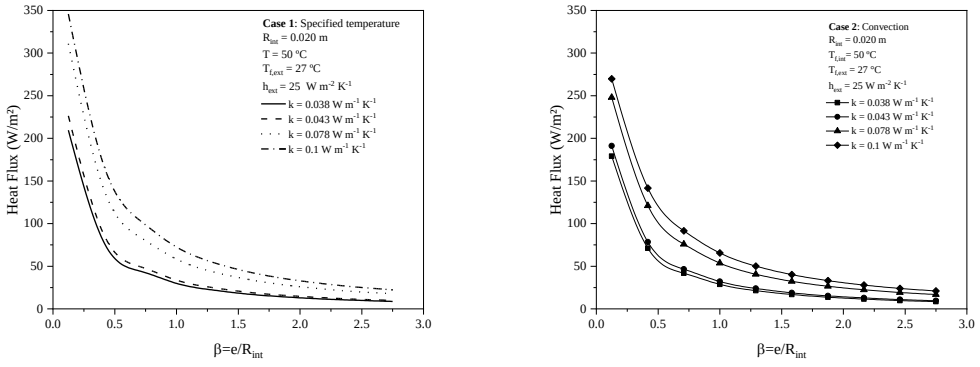

(a) (b)

Figure 10. Influence of β on the heat flux on the external surface for different convective coefficients and thermal conductivities for $h_{ext} = 25\ W/(m^2 \cdot K)$: (a) Case 1; (b) Case 2 (Authors, 2023).

Figures 11a and 11b illustrate the heat transfer rate per unit length, while Figures 11c and 11d show the heat flux on the external surface in relation to β for $k = 0.078\ W/m \cdot K$ and three distinct external heat transfer coefficients (2, 16, and 25 W/m²·K). In Figures 11a and 11b, it is observed that, in the only condition where the β_{cr} is present, with $h_{ext} = 2\ W/m^2 \cdot K$, the heat transfer rate presents reduced values for both Case 1 and Case 2. This occurs even in the range of β values where there is a tendency for increased heat exchange in the insulator, as indicated in Figure 8a. For the other scenarios, with, $h_{ext} = 16\ W/m^2 \cdot K$ e $h_{ext} = 25\ W/m^2 \cdot K$, the effectiveness behavior of the insulator is noticed for any β value. It is noted that the values of heat exchanges per unit length tend to approach for high β values, regardless of the h_{ext}, values, suggesting a trend of insulator thickness independence in influencing the amount of heat exchanged between the internal and external regions of the piping. Such behavior can also be analyzed from the perspective of heat flux, as shown in Figures 11c and 11d, where the heat flux values for high β values tend to converge for all h_{ext},values.

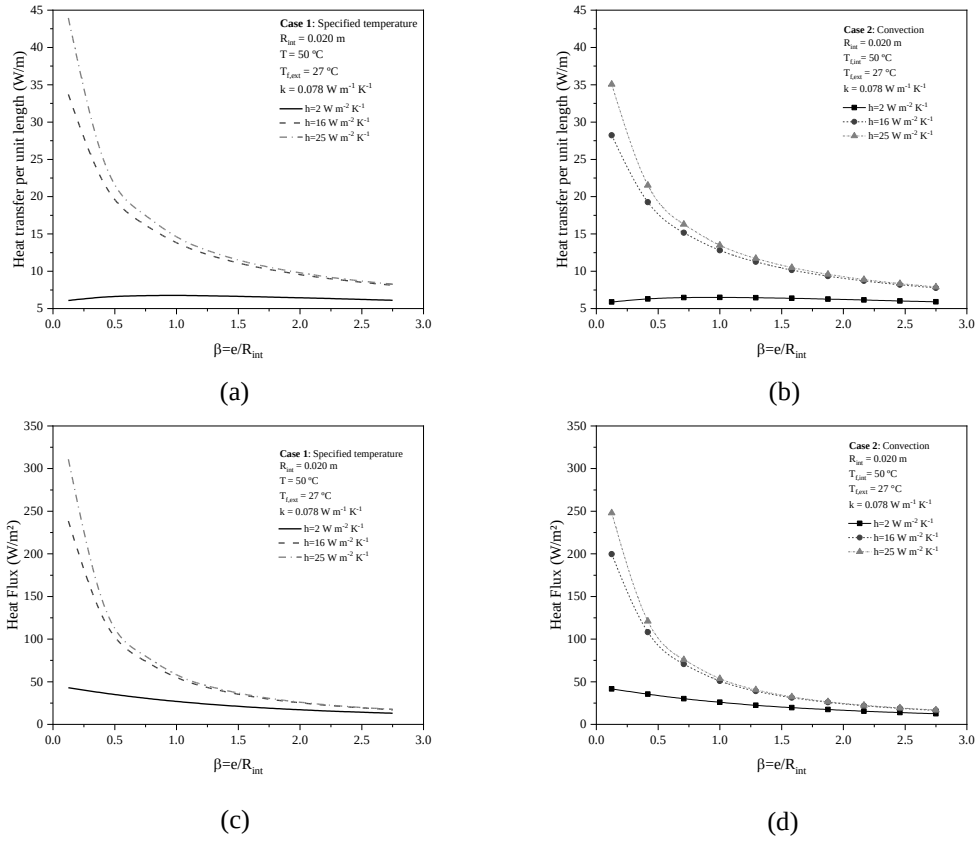

Figure 11. Influence of β on the heat transfer per unit length and the heat flux on the external surface considering various convective coefficients and thermal conductivity k = 0.078 W/m·K: (a) heat transfer per unit length for Case 1; (b) heat transfer per unit length for Case 2; (c) heat flux for Case 1; (d) heat flux for Case 2 (Authors, 2023).

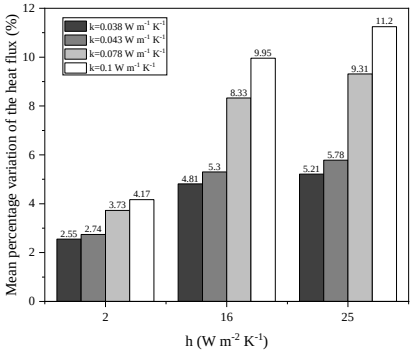

Figure 12. Mean percentage variation of the heat flux on the external surface values between Case 1 and Case 2 (Authors, 2023).

In Figure 12, the mean percentage variation of the heat flux on the external surface values between Case 1 and Case 2 is presented. An increasing trend of this mean is observed with the rise in thermal conductivity k for all indicated convection coefficients h.

Based on the analysis conducted, the results suggest that in situations with low convective coefficients and insulating materials of low conductivity, assuming the fluid temperature to be the same as the wall temperature (and *vice versa*) results in a discrepancy of 2 to 11%, approximately, in the heat flux calculation. In certain practical contexts, this variation is acceptable and can be adjusted in the safety factor calculation of the project. Therefore, in similar scenarios where the fluid or wall temperature is not available, it is feasible to consider them equivalent without incurring significant errors in the heat flux calculation.

5. CONCLUSIONS

In this work, the mathematical and numerical modeling of steady-state heat diffusion in cylindrical thermal insulators was performed using the finite volume method and implemented in the Matlab software. The results highlighted the utility of the radius ratio (β) in thermal insulation efficiency analysis. The study of heat flux and the effects of insulation thickness were based on the value of β and the critical radius ratio (β_{cr}).

It was observed that only three scenarios yielded $\beta_{cr} \geq 0$, highlighting situations that need careful examination because of the potential for undesired increased heat transfer in insulated tubes. As β increased, the temperature distribution on the tube's external surface displayed a nonlinear profile. The study also looked at how heat flux changes with different β values, thermal conductivity, and external heat transfer coefficient. Additionally, it was found that equating the fluid temperature with the wall temperature (and *vice versa*) can be considered acceptable in specific practical contexts, and adjustments can be made in the calculation of the project's safety factor.

Through this study, the importance of the critical insulation thickness and its application in the optimization process of insulation material thickness or the determination of compatibility between a coating and a material was understood. The proposed methodology can serve as a basis for future research involving the analysis of ideal insulation thickness in different geometries and operating conditions.

6. REFERENCES

Anisimova, E Yu. "Methodology for Calculating the Ineffective Diameter of Thermal Insulation." IOP Conference Series. Materials Science and Engineering 962.3 (2020): 32001. Web.

Çengel, Y.A.. “Transferência de Calor e Massa – Uma abordagem prática”, Mc. Graw Hill, São Paulo, 3ª ed., 2009;

Kaynakli, O., 2014. "Economic Thermal Insulation Thickness for Pipes and Ducts: A Review Study." Renewable & Sustainable Energy Reviews 30 (2014): 184-94. Web.

Li, Wang, Bo Yu, Xinran Wang, Peng Wang, and Shuyu Sun. "A Finite Volume Method for Cylindrical Heat Conduction Problems Based on Local Analytical Solution." International Journal of Heat and Mass Transfer 55.21-22 (2012): 5570-582. Web.

Maliska, C.R. Transferência de Calor e Mecânica dos Fluidos Computacional. Rio de Janeiro: LTC – Livros Técnicos e Científicos Editora, 1995, 424p

Powar, S. B., and Dhamangaonkar, P.R. "Estimation of Critical Thickness of Insulation for Regular Polygon Cross-section Ducts/conductors." Materials Today : Proceedings (2022): Materials Today : Proceedings, 2022. Web.

Patankar, S.V.” Numerical Heat Transfer and Fluid Flow” Hemisphere Publishing Co., 1980.

Shi, Jinsheng, and Qiaozhen Zhang. "An Approximate Analysis of Insulation Thickness of Elliptic Pipe." IOP Conference Series. Earth and Environmental Science 555.1 (2020): 12119. Web.

Usman, M., & Kim, Y. K. (2022). Pipe Insulation Evaluation for Low-Temperature District Heating Implementation in South Korea. Frontiers in Energy Research, 9, 793557.

Versteeg, H.K., Malalasekera,W. An Introduction to Computational Fluid Dynamics – The Finite Volume Method. Person Prentice Hall, 2º ed, 2007.

Zarubin, V. S., G. N. Kuvyrkin, and I. Yu Savel’eva. "Critical and Optimal Thicknesses of Thermal Insulation in Radiative-convective Heat Transfer." High Temperature 54.6 (2016): 831-36. Web.

7. RESPONSIBILITY NOTICE

The authors are the only responsible for the printed material included in this paper.